Polar Geosci., **14**, 195–211, 2001

P-wave velocity structure of the ice sheet and the shallow crust beneath the Mizuho traverse route, East Antarctica, from seismic refraction analysis

Tomoki Tsutsui[1], Hiroshi Murakami[2], Hiroki Miyamachi[3], Shigeru Toda[4] and Masaki Kanao[5]

[1]*Faculty of Engineering and Resource Science, Akita University, Akita 010-8502*
[2]*Technical Center for Seismological Observations, 2-6-20, Amakubo, Tsukuba 305-0005*
[3]*Faculty of Science, Kagoshima University, Kagoshima 890-0065*
[4]*Faculty of Education, Aichi University of Education, Kariya 448-0001*
[5]*National Institute of Polar Research, Kaga 1-chome, Itabashi-ku, Tokyo 173-8515*

Abstract: A seismic survey with a high density network was conducted by the 41st Japanese Antarctic Research Expedition (JARE-41) in the austral summer of 1999–2000. The seismic line was 190 km long, along the Mizuho traverse route from the base camp S16. 160 temporary seismic stations using data loggers were installed. The first arrival times were analyzed by the refraction method. The structure of the upper crust and overlying ice-sheet are revealed down to 7 km from refraction analysis of the first arrival times. A three layered structure is estimated. The first layer with a velocity of 3.8 km/s appears to be ice-sheet. The second layer with a velocity of 6.2 km/s of *P*-wave velocity is the surface layer of the continental crust. The thickness of this second layer is estimated to be approximately 5 km. The third layer is defined by the *P*-wave velocity of 6.5 km/s. Its shape of the upper interface is not declared. The topography of the basement determined from seismic refraction matches well with that determined from ice-radar sounding except for a small difference in the estimated depth of the basement. Two abrupt changes of the second layer depth are found near shot S-1 and shot S-4. The former includes a velocity change in the second layer. The latter discontinuity corresponds to the echo-less points of the ice-radar sounding. Velocity changes in the first and second layers are not detected across the latter discontinuity.

key words: seismic survey, Mizuho traverse route, Enderby Land, ice-sheet thickness, top crust

1. Introduction

Enderby Land located in the eastern Antarctica, where the Japanese Antarctic Research Expeditions (JARE) have worked frequently, contains the Napier Complex as its central zone, surrounded by Proterozoic and Paleozoic complexes. The Lützow-Holm Bay area, where Syowa Station is located, experienced igneous interaction before 500 Ma (Hiroi *et al.*, 1991; Shiraishi *et al.*, 1994). Geologic research has revealed that parts of this area may have different metamorphic histories. Moreover, it is probable that details of the subsurface structure in this area involve cumulative remnants of ancient geological

processes (Kanao, 1997).

However, the thick ice-sheet over the continental crust prevents us from directly observing geological features of the crust in detail. Only geophysical approaches, such as the seismic method and gravity surveys, can be used to determine the subsurface structure. Surface correction in terms of deep seismic analysis is needed in order to discuss the detailed structure.

Ice-radar sounding has recently become a popular method to determine the thickness of the ice-sheet. Ice-radar sounding along the JARE traverse routes has revealed distributions of ice-sheet thickness that are not uniform and gradually increase inland (*e.g.*, see Kamiyama *et al.*, 1994; Fujita *et al.*, 1999). Ice-radar results, however, describe the depth of electro-magnetic structures as a distribution of echoes, not the exact distribution of seismic velocity. Therefore, new seismic surveys can reveal the velocity distribution in the ice-sheet more precisely than those made before.

JARE-20, -21 and -22 carried out seismic operations for the deep crustal survey along the Mizuho traverse route (Ikami *et al.*, 1983; Ito *et al.*, 1983). The operation used chemical explosive as the seismic source and reported the velocity structure down to the Moho discontinuity (Ikami and Ito, 1986). The survey was the best up until that time, but only stations with 10 km spacing were available. Therefore only limited information about ice-sheet thickness was obtained.

After that survey, there was a long blank until the next chance for such a survey by JARE. JARE-41 seismic operation during austral summer of 1999–2000 was conducted along the Mizuho traverse route again as a part of the Structure and Evolution of East Antarctic Lithosphere (SEAL) transect project. The purpose of this operation was to obtain a more precise structure than those estimated by JARE-21 and -22, taking advantage of the improved technology of the recording apparatus. The details of this operation have been described in Miyamachi *et al.* (2001) and Murakami *et al.* (2001). This paper describes the result of refraction analysis of the first arrivals (Miyamachi *et al.*, 2001) and the distribution of ice-sheet thickness along the seismic line.

2. Seismic survey and data

The seismic line obtained by JARE-41 is shown in Fig. 1. The seismic line is extended up to 190 km along the Mizuho traverse route from the base camp at point S16. 160 temporary seismic stations were spread out. A recording system for a station consists of a single component seismometer (model L22D with 2 Hz natural period for vertical motion type by MarkProducts Co.) and a stand-alone seismic recorder (LS8000SH 20 Mbytes capacity by Hakusan Industry Co.). A Cyclone battery (6V 16Ah) was used as the power source for the recorder. The seismic recorder and the battery are stored in a plastic container with heat insulation. Each station is programmed to have three data acquisition windows and five time-base calibrations with a built-in GPS receiver for one day. Data acquisition and storage were done on site. The recorders ran for 28 days at maximum.

Locations of the stations were measured with precise GPS receivers (Ashtech Z-FX) after the deployment of instruments. Exact locations of the stations are given in Miyamachi *et al.* (2001). All stations were retrieved after completion of all shots and

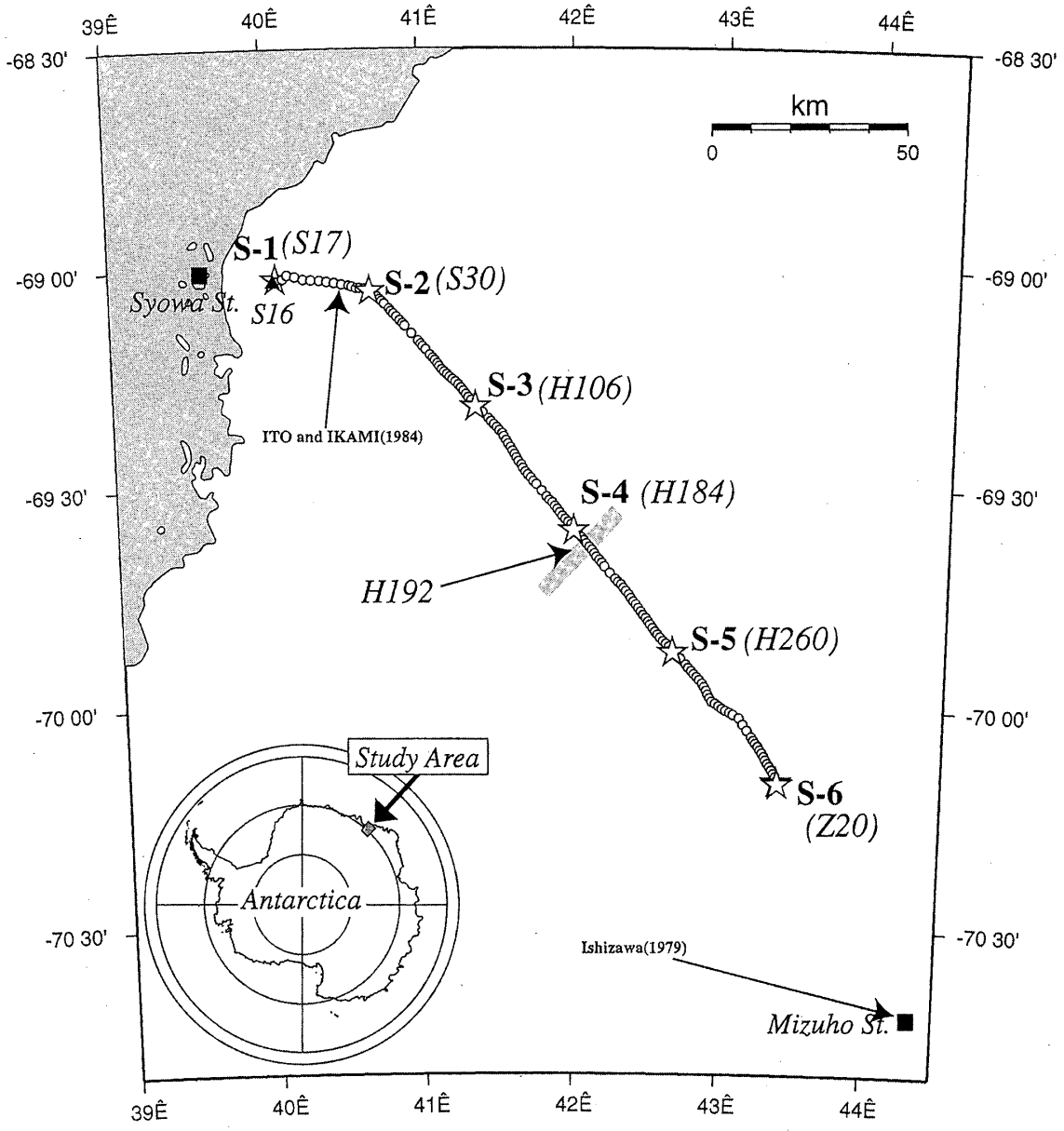

Fig. 1. JARE-41 seismic line; open stars mark seven shot points and open circles indicate 160 seismic stations except for the line-up stations near the each shot point. Distances between neighboring shot points are approximately 40 km except for the distance between shot points S-1 and S-2 which is 26 km. Important places are marked with arrows and the discontinuity is marked by the band at H192.

then data were transferred from the recorders to hard disk in a PC on the return trip to Japan.

Figures 2 to 7 show record sections with detected first arrivals for shots S-1 to S-6, respectively. The common legend of these figures is as follows: the abscissa denotes distance from the shot point in km. The vertical axis denotes reduced travel time with a reduction velocity 6.2 km/s. Solid symbols at the onset of the waveform indicate the time of the first arrival. Large, medium and small solid circles in Figs. 2 to 7 mark detected arrivals with quality ranks A, B, C, respectively. Solid triangles in these figures describe

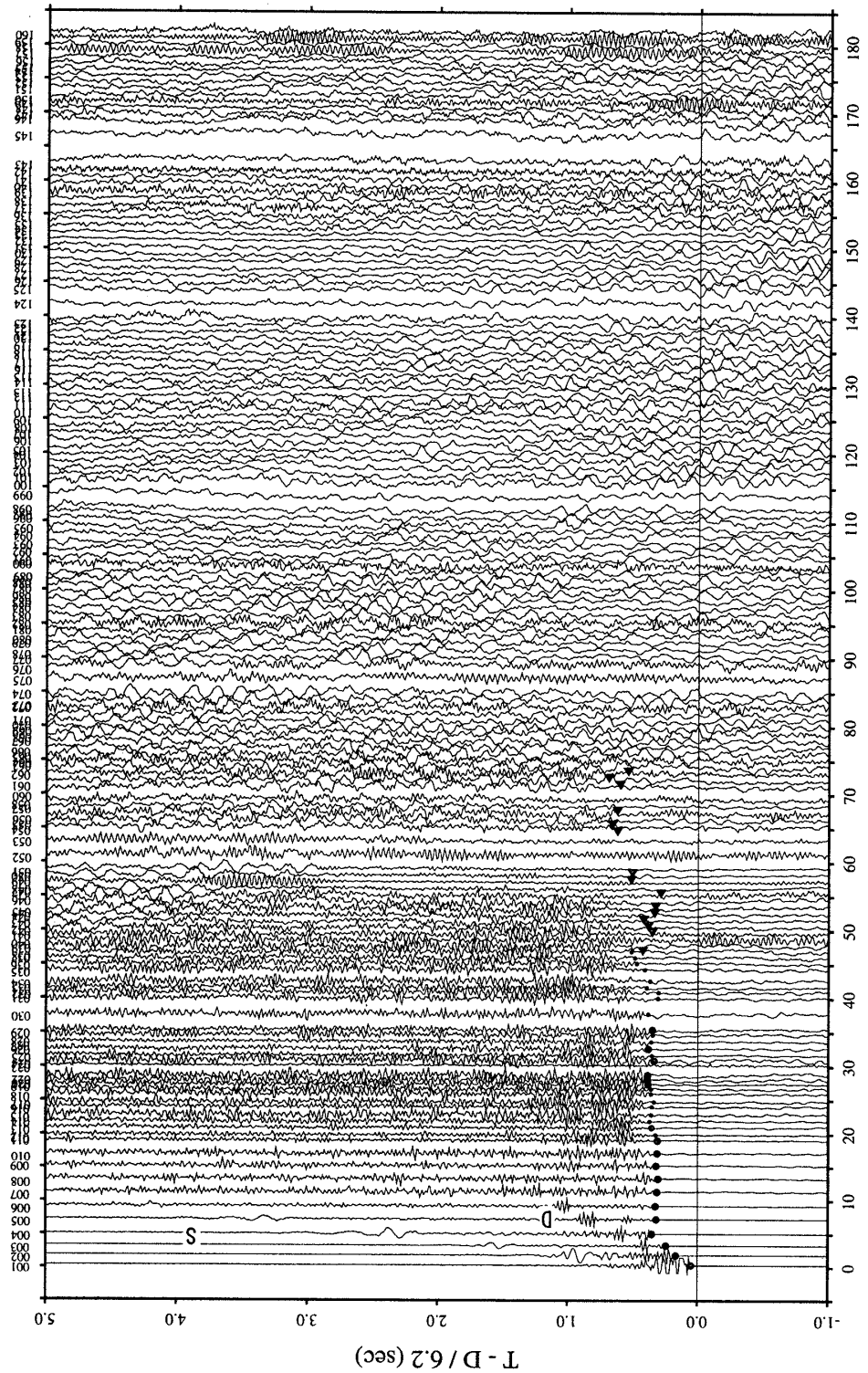

Fig. 2. Shot record and detected first arrivals for shot point S-1: The abscissa describes the distance from the shot point in km and the vertical axis describes the reduced travel time in seconds for the velocity 6.2 km/s. The labels on the top of each seismograph are the station codes for the corresponding stations. "D" indicates the direct wave and "S" indicates the surface wave. Detected first arrivals for each station are indicated by solid symbols. Sizes and types of solid symbols are described in the text.

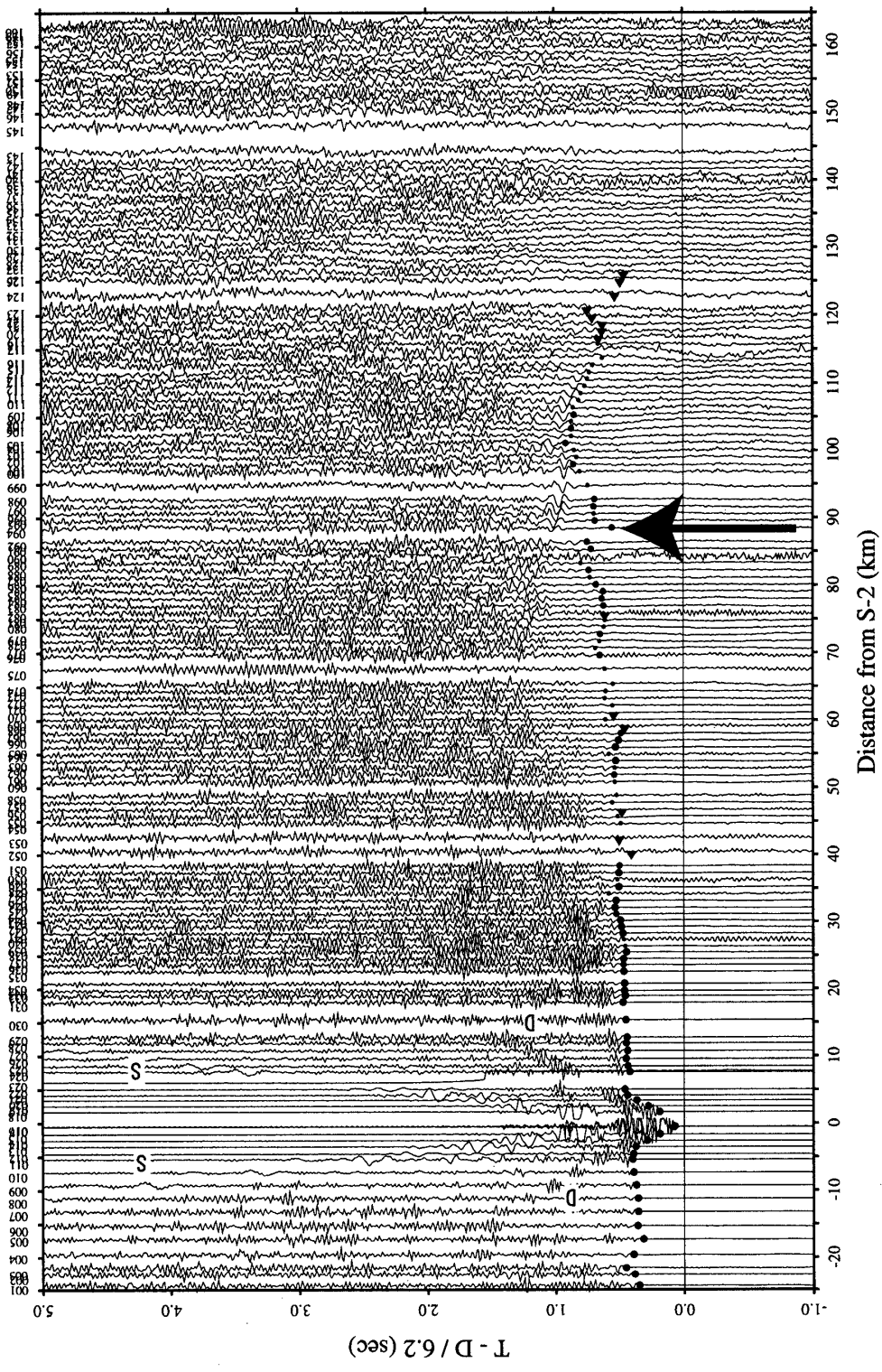

Fig. 3. A shot record and detected first arrivals for shot point S-2: The symbols have the same meanings as in the previous figure. The first arrivals can be detected in the distance range over 100 km from the shot point. In the farther range over 100 km, faster apparent velocity appears.

detected arrivals with quality rank L. Definitions of these quality ranks are as follows (Miyamachi *et al.*, 2001): rank A is defined with an accuracy range is smaller than or equal to 0.015 s; rank B with an accuracy between 0.015 s and 0.030 s; rank C with an accuracy range beyond 0.030 s with detectable polarity, and rank L with an accuracy range beyond 0.030 s without detectable polarity.

Figure 2 is a record section for shot S-1 at point S17. Clear onsets can be detected up to 45 km from the shot. The apparent velocity of 4.7 km/s appears up to 5 km, and the much higher velocity of 6.2 km/s at farther stations.

Figure 3 is a shot record for shot point S-2 at point S30. The apparent velocity of 3.8 km/s is observed within 5 km from the shot point. The apparent velocity of 6 km/s is observed in the stations on the right side, and higher apparent velocity on the left side of the shot point. Moreover, a portion with larger apparent velocity appears beyond 100 km on the right side. An undulation of the first arrival observed around 90 km from the shot point is marked with an arrow.

Figure 4 is a shot record for shot S-3 fired at point H106. The apparent velocity of 3.8 km/s is observed within 6 km from the shot point. The near field velocity of 3.8 km/s and difference of apparent velocity across the shot point are the same as those of other shots. A higher apparent velocity than 6.2 km/s is observed on the left side of the shot point S-3, while a lower apparent velocity appears on the right side. An undulation of the first arrival is also observed at 50 km from the shot point as marked with an arrow.

Figure 5 is a shot record for shot S-4 at point H184. The appearance of the first arrivals near the shot point is the same as those of other shots. The difference of apparent velocity across the shot point is not clear in this figure. However, the difference of the intercept times up to 0.2 s between both sides is significant.

Figure 6 is a shot record for shot S-5 at point H260. The same distribution of the segments of travel times with apparent velocities 3.8 km/s and 6.2 km/s appears as for other shots. A travel time gap is indicated with an arrow around −30 km from the shot point.

Figure 7 is a shot record for shot S-6 at point Z20. The apparent velocity of 3.8 km/s is observed in the near field, and 6.2 km/s at farther distance up to 70 km from the shot point. The travel time gap is also found around −70 km. A much higher apparent velocity of 6.5 km/s can be observed beyond 70 km from the shot point, with significant delay time at the travel time gap.

A well-developed later phase appears at distances over 80 km in Figs. 6 and 7. These later phases are marked with bars in each figure. An outstanding feature of the later phases is a predominant low-frequency component around 8 Hz. These later phases are interpreted as reflections from the deep crust. Tsutsui *et al.* (2001) describe reflection analysis of the well-developed later phases.

In addition, a clear dispersed surface wave can be observed around the shot points in Fig. 4. The same wave packets also appear in Figs. 5 to 7 as in Fig. 4. These are marked with "S" in each figure. Analysis and discussion of the surface wave will be given in a forthcoming paper.

All the detected first arrivals within 20 km range are plotted against the distance from each shot point in Fig. 8. A common apparent velocity of 3.8 km/s is found for all shots except for the travel time curve of shot S-1. An exceptions is the apparent velocity

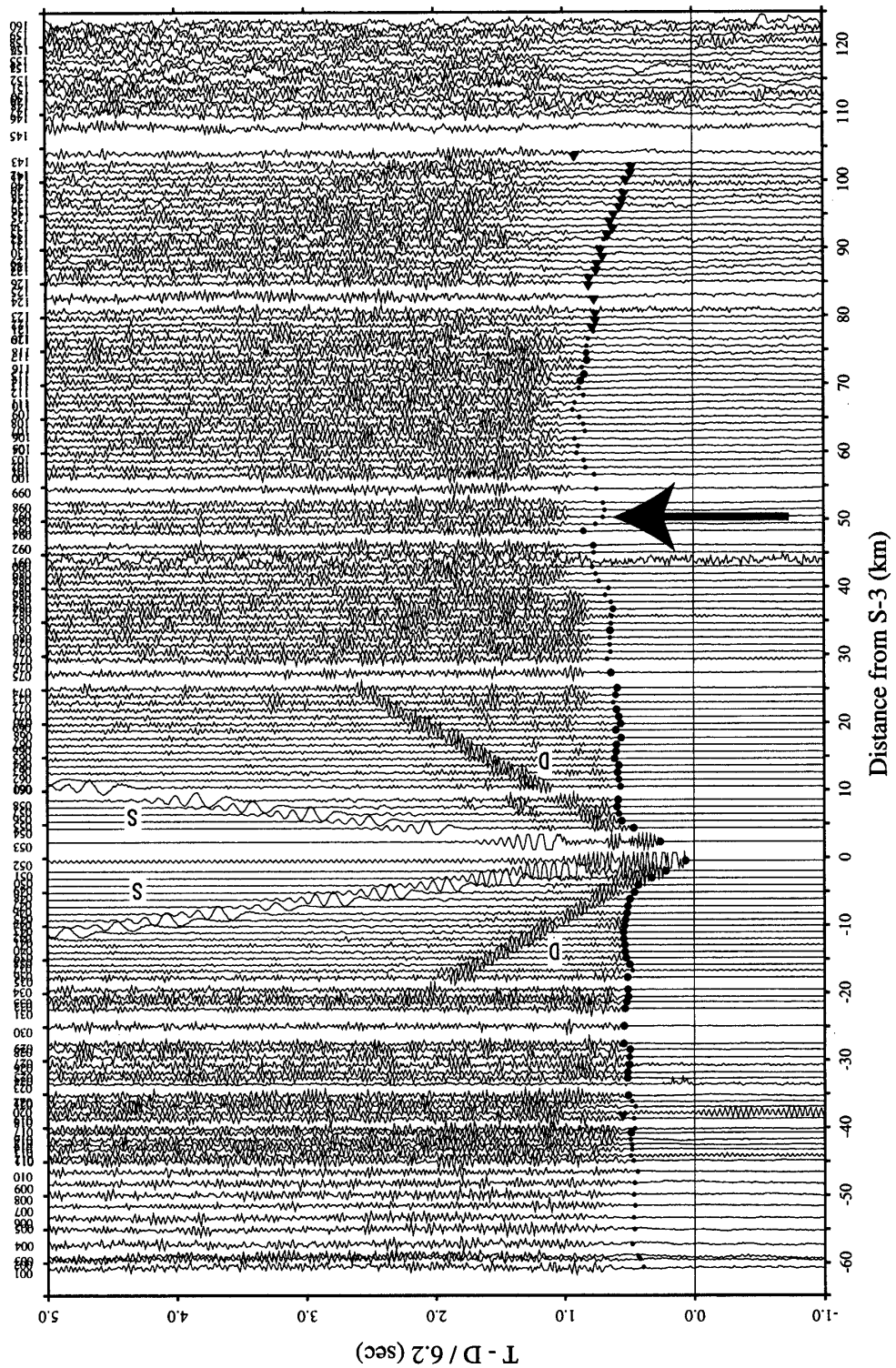

Fig. 4. Shot record and detected first arrivals for shot point S-3: The symbols have the same meaning as in Fig. 3. The first arrivals are detected in the distance range over 100 km from the shot point. The thick arrow indicates a gap of the travel time.

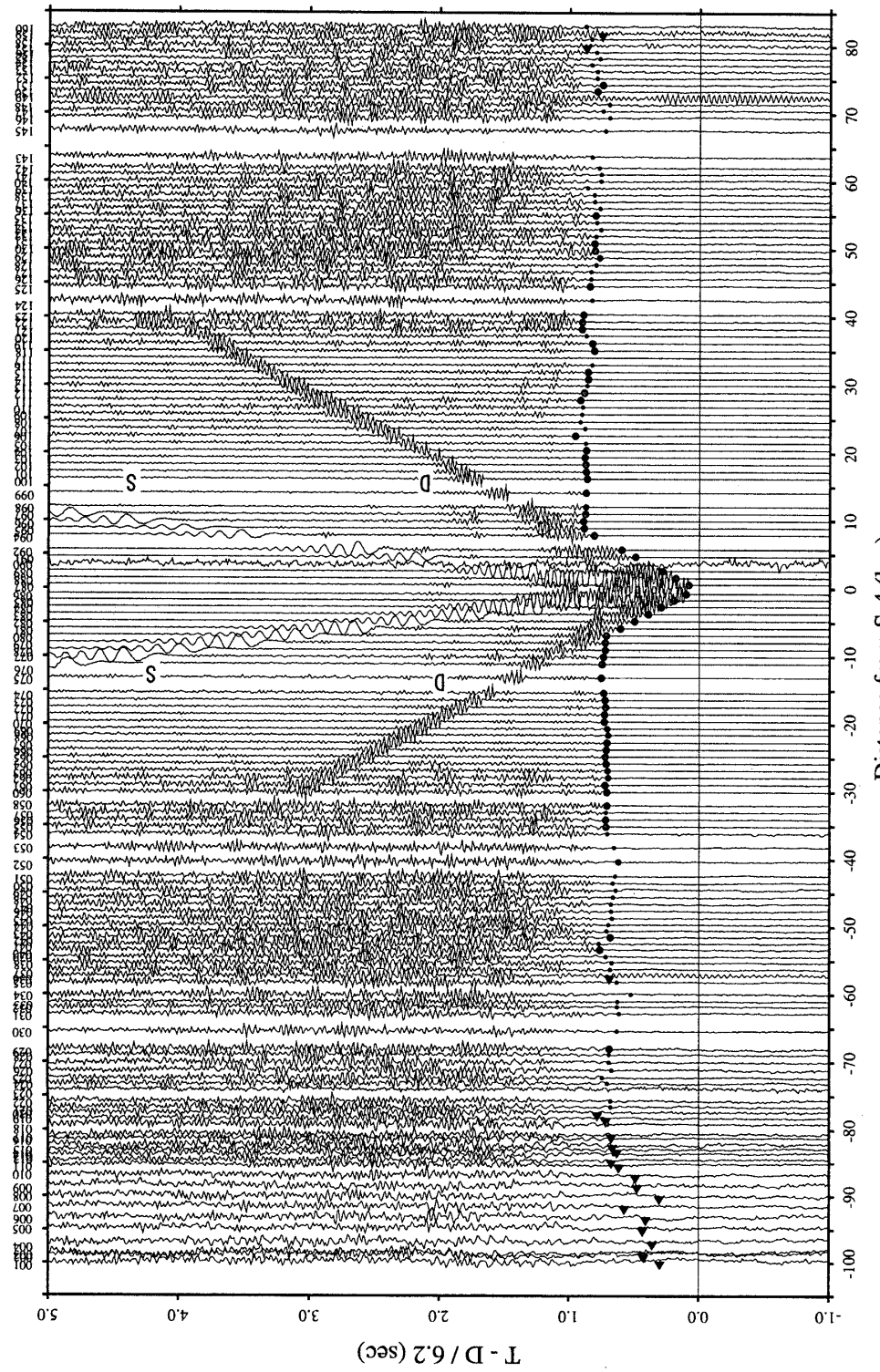

Fig. 5. Shot record and detected first arrivals for shot point S-4: The same symbols as in Fig. 4 are applied. The first arrivals can be detected up to the distance range beyond 100 km from the shot point. A significant difference in the intercept times can be observed on the both sides of the shot point.

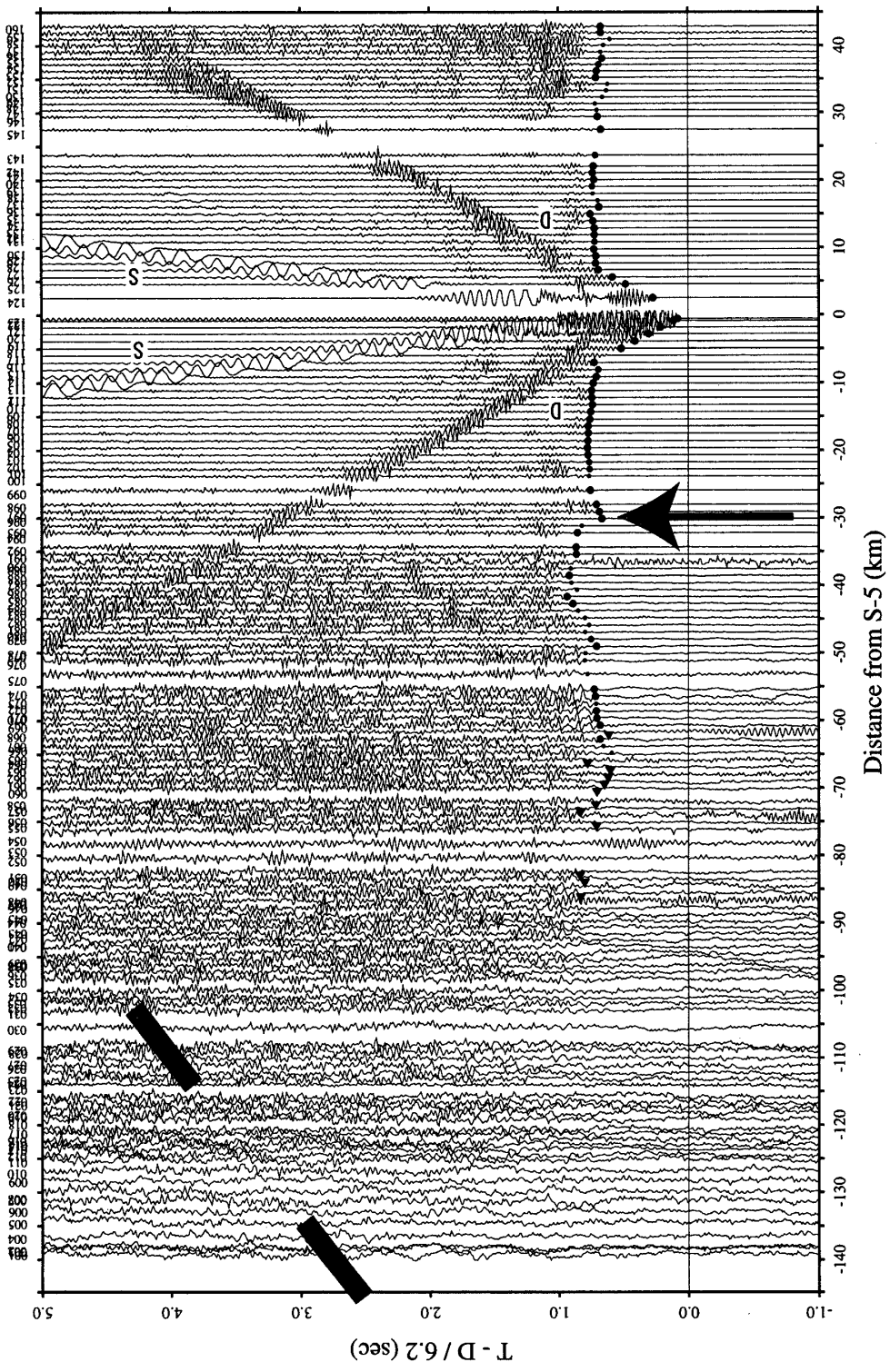

Fig. 6. Shot record and detected first arrivals for shot point S-5: The same symbols as in Fig. 5 are applied. The first arrivals can be detected up to the distance range over 100 km from the shot point. Clear direct arrival for the first layer and surface wave phase also develop in this figure. A significant gap in the delay time can be clearly observed near the shot point S-4. Thick bars indicate a later phase.

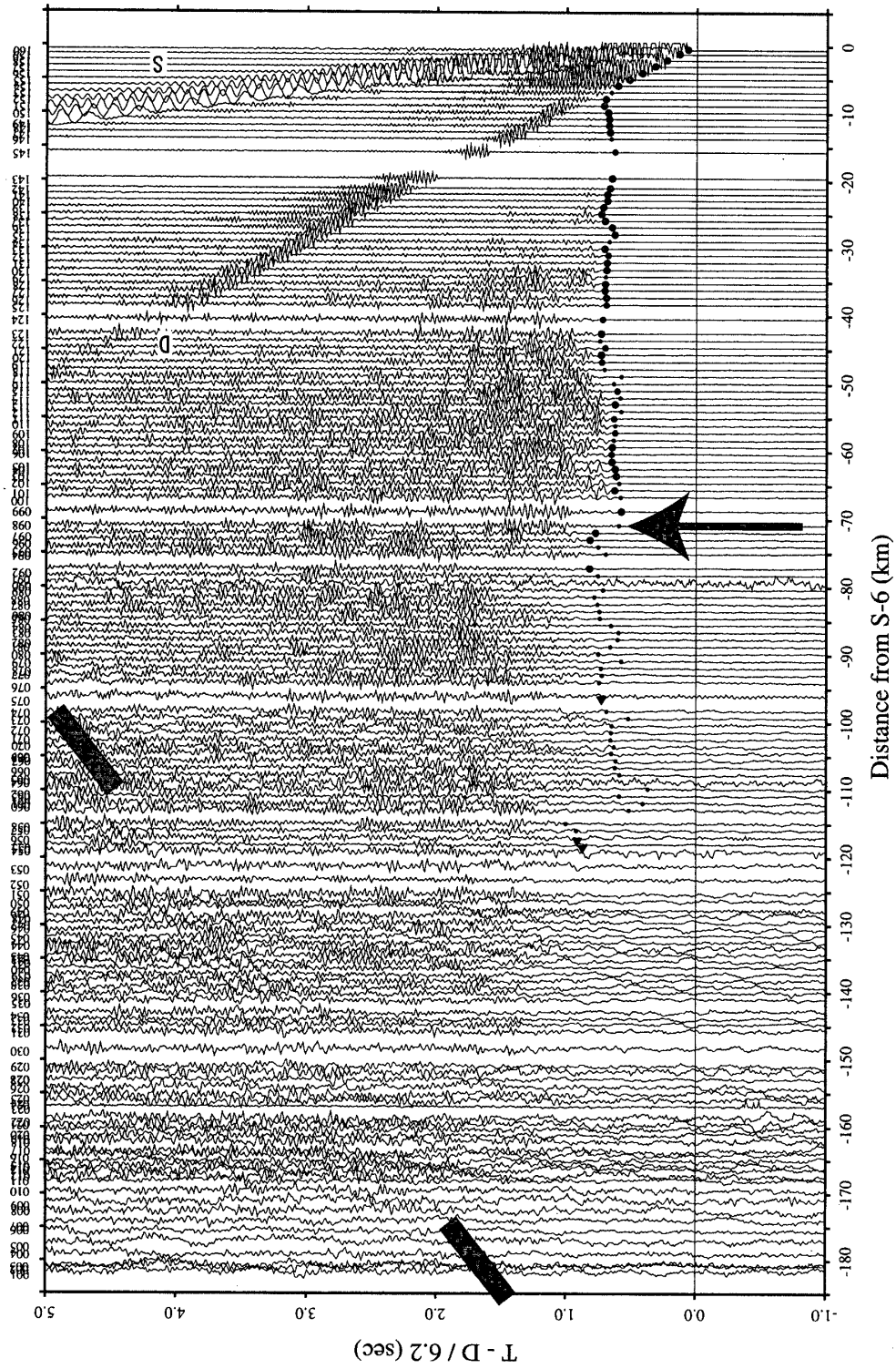

Fig. 7. Shot record and detected first arrivals for shot point S-6: The same symbols as in Fig. 6 are applied. The first arrivals can be detected up to the distance range over 100 km from the shot point.

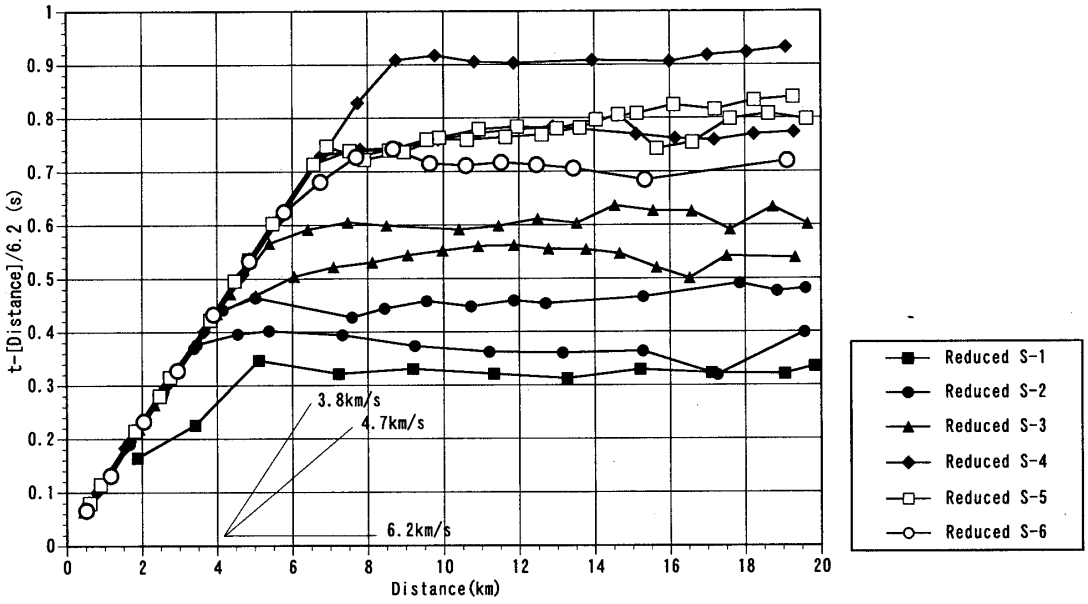

Fig. 8. The first arrival distribution for the shot distance: The abscissa describes the source distance in km and the vertical axis describes the travel time in seconds. The same apparent velocity 3.8 km/s can be observed in the near field among shot points S-2 to S-6. Near field travel times for shot point S-1 are the exception, with an apparent velocity of 4.7 km/s. The intercept time increases inland.

of 4.7 km/s which appears before the appearance of 6.2 km/s for shot S-1. In addition, the intercept time becomes larger toward Mizuho Station, except for that of the shot 4. The largest intercept time appears in the one side of the travel time curve of shot S-4.

3. Analysis and results

Two types of travel time curves are classified in Fig. 8 on the basis of the near field apparent velocity as follows. The first type has a bend within 5 km from the shot point, with an apparent velocity of 3.8 km/s in the near field segment. Travel time curves of shots S-2 to S-6 are of the first type. The second type also has a bend in the near field but an apparent velocity of 4.7 km/s appears in the near field. The travel time curve of the shot S-1 is the second type.

Figure 9 shows travel time curves for all shots which placed at the corresponding shot points along the JARE-41 seismic line. A travel time gap near shot S-4 is indicated with vertical solid arrows. This travel time gap implies an abrupt change in the thickness of the 3.8 km/s layer.

General features of the travel time curves in Fig. 9 are single or double bends. These bends are indicated with open triangles in the figure. These features, suggest that two or three layer structure analysis is appropriate for the data set. Hereafter the method of difference (Hagiwara, 1938) , one type of refraction analysis, is applied to the data.

In the first stage, the JARE-41 seismic line is split into segments with the pair of closest shot points used for the first layer analysis. These segments are labeled "For Base altitude 1" below the travel time curves in Fig. 9. The next stage, a different segment with a pair of the next closest shot points is used for the analysis. These segments are

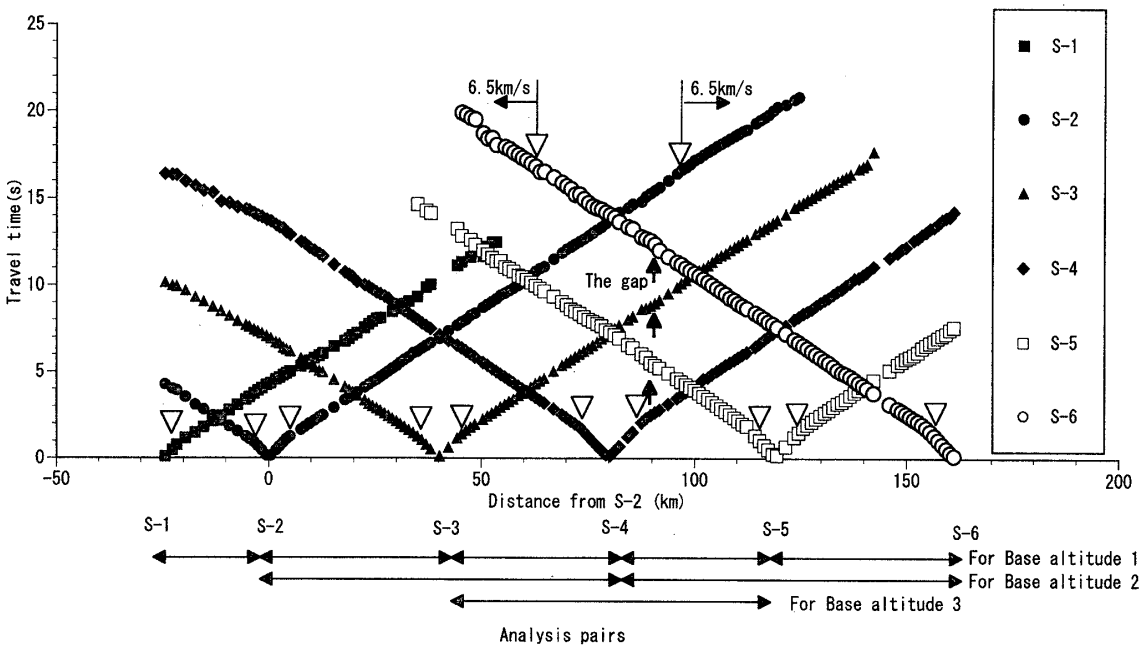

Fig. 9. Distribution of the travel time curves along the JARE-41 seismic line: The abscissa describes the route distance from shot point S-1 in km and the vertical axis denotes the travel time in seconds. Origins of each travel time curve are placed for the corresponding shot point. Bends of the travel time curve are marked with open triangles. A gap can be observed near S-4; it is indicated with thick arrows.

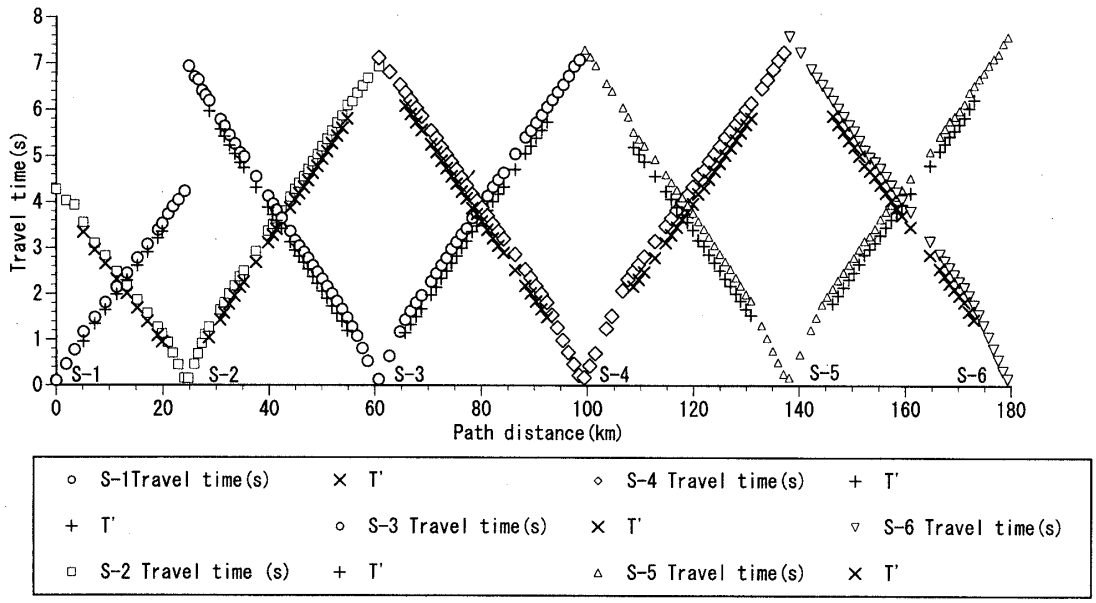

Fig. 10. Estimated equivalent travel time curves and raw travel time curves: Symbols "X" denote raw travel times of the first arrival. Symbols "+" denote estimated equivalent travel times. No clear velocity variation can be observed on the both sides of shot point S-4.

described as "For Base altitude 2" and "For Base altitude 3" below the previous diagram in Fig. 9. The appropriate pair of shots, S-2 and S-6, is selected for analysis of the third-layer.

Figure 10 shows all raw travel time curves with the equivalent travel time curves for the neighboring shot pair which are described by "For Base altitude 1" in Fig. 9. The equivalent travel time curves, "T'", are linear with a constant velocity of 6.2 km/s. This simple appearance of the equivalent travel time curves shows small velocity variations in the second layer. It is inferred that a 3.8 km/s layer overlays a 6.2 km/s layer. The difference between the raw travel time and the equivalent travel time is the so-called delay time and is proportional to the thickness of 3.8 km/s layer. The estimated topography of the bottom of the first layer is labeled "Base altitude 1" in Fig. 11. Each result for the pair is shown with different symbols in this figure. The final result is labeled "Altitude (Final)" which is an average among the results for "Base altitude 1" to "Base altitude 2" and a part of "Base altitude 3" which have a regular value.

Steep abrupt changes in the thickness of the first layer are revealed at 5 km and at 110 km from shot S-1 as shown in Fig. 11. The former corresponds to the exceptional behavior of the travel time around shot S-1, and the latter corresponds to the travel time gap or undulation that appears in the shot records (Figs. 4 to 7) around shot S-4. A trough-shaped bottom of the first layer is observed on the coastward side of the steep change.

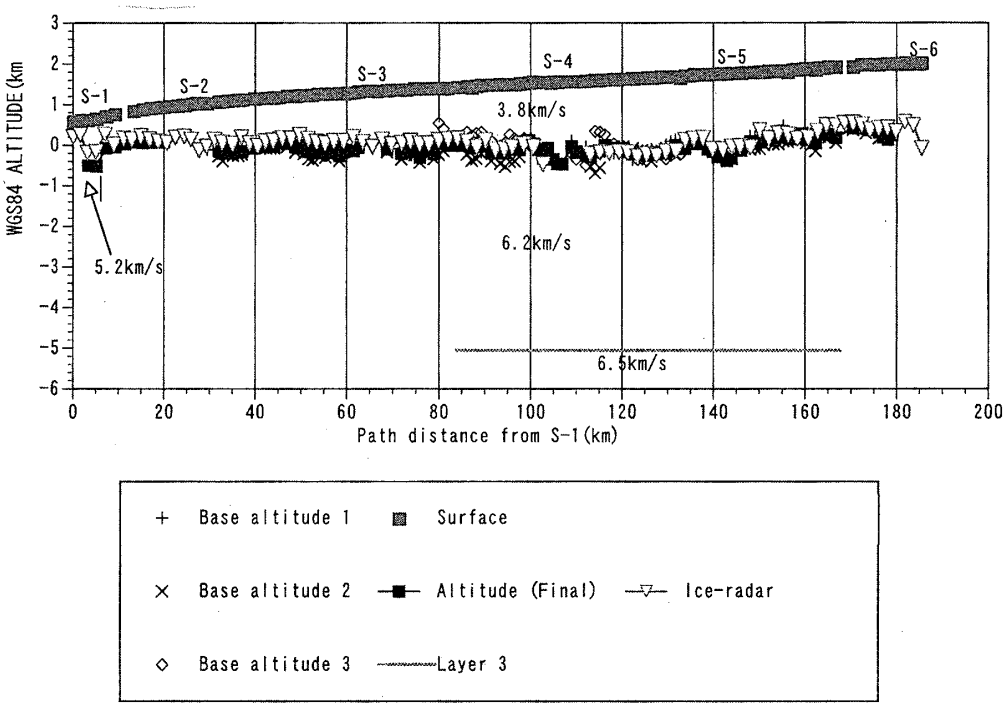

Fig. 11. Estimated velocity structure beneath the JARE-41 seismic line: The abscissa describes the route distance from shot S-1 and locations of the shot points are labeled. The vertical axis describes elevation above the sea level defined with WGS84 coordinate. The topmost curve is the surface of the ice-sheet. The results are plotted and labeled with "Base altitude 1" to "Base altitude 3" and "Altitude (Final)" for the bottom of the first layer. The upper face of the third layer is labeled "Layer 3". The ice-radar sounding by Kamiyama et al. (1994) is plotted by open triangles.

The thickness distribution of the 3.8 km/s layer can be divided into two portions at the discontinuity near shot S-4: The first portion ranges up to the distance of 110 km from shot S-1, and the second is the rest of the seismic line. The layer thickness gradually thickens inland and the bottom of the first layer (the 3.8 km/s layer) is estimated to be around sea level in the first portion. The layer thickness is approximately constant and the bottom of the first layer rises gradually toward shot S-6 in the second portion.

The 3.8 km/s layer corresponds to the ice-sheet according to the research of Ishizawa (1979) at Mizuho Station. He determined the velocity structure in the ice-sheet down to 100 m depth by using refraction at the surface, referring to the core sample. The result of his refraction survey and the measurements of seismic velocity for the core samples agree with each other. Ishizawa (1979) showed that the seismic velocity increases rapidly down to 20 m depth and then converges into 3.8 km/s. Thus the first layer with the velocity of 3.8 km/s corresponds to the ice-sheet. The velocity of the first layer is uniform as shown in Fig. 9.

The second bend in the travel time curves for the shot points S-2 and S-6 appears in the range over 100 km from the shot point in Fig. 9. These bends are marked by open triangles in Fig. 9. The segments farther than the markers have a higher apparent velocity around 6.5 km/s. This fact reveals that the third layer is detectable. Because both third segments have the same apparent velocity and the accuracy of the detected first arrivals is not enough in this range, only horizontal layer analysis is appropriate.

The final result for the third layer is labeled "Layer 3" in Fig. 11. The boundary of the third layer is inferred to be around 5 km below sea level; its topography is unclear.

4. Discussion

4.1. Comparison with other results

The result of the ice-radar sounding (Kamiyama *et al.*, 1994) is plotted in Fig. 11 with open triangles. Overall features of the echo from the bedrock look the same as "Altitude (Final)" of the seismic results. However, the seismic result shows the bedrock being deeper than the ice-radar. A systematic difference appears clearly in the section between shots S-2 and S-4. The maximum difference between both results is approximately 0.3 km.

Several possible reasons for this discrepancy are as follows: 1) difference of the reference elevation of the measurements, 2) seismic velocity variation in the first layer, and 3) difference in the resolution of the methods. For the first possibility, a bias of elevation from the difference of the reference is included in the plot of Fig. 11 because not all survey points of both studies are the same. However, the bias is estimated to be 40 m higher for the JARE-41 surface on an average than that of Kamiyama *et al.* (1994). Therefore the bias of the surface elevation cannot explain the difference of the basement depth.

Next, if the velocity variation in the first layer exists in this section, the difference in the basement depth requires more than 10% of the velocity variation in order to explain the difference in thickness. The constant apparent velocity of 3.8 km/s is observed in the near field for the corresponding shots S-2, S-3 and S-4 in Fig. 8, and the change in

velocity by 10% is impossible to determine from the data. The velocity variation is not also reasonable for the cause of the difference in thickness.

Finally, let us consider the difference of resolution between the two methods. The resolution of the ice-radar sounding is in the range of 5–85 m. The resolution of the seismic refraction in the present study is in the range of 100–350 m. The difference of resolution between the two methods should be noted. The estimated basement depth obtained by the ice-radar sounding varies in the short spatial period in the section between shots S-1 and S-4, and varies over a longer period in the section between shots S-4 and S-6. Good coincidence between the seismic result and the ice-radar result is found in the latter section. Accounting for the resolution, seismic refraction is insensitive to such a short period variation of the basement elevation. Thus it is concluded that the seismic result describes the average thickness of the ice-sheet; while the ice-radar result describes only local topography within the range of transmitted wavelength.

4.2. Discontinuity in the second layer near shot point S-1

An exceptional apparent velocity of 4.7 km/s is observed only in the near field of shot point S-1. Because a significant delay is also observed at the corresponding stations in the reverse shot S-2 (Fig. 2) as well as shot S-1, the segment with 4.7 km/s appears to be a low velocity portion of the basement layer. A corresponding second layer defined by a velocity of 5.2 km/s is estimated to exist near shot S-1 in Fig. 11.

A previous exploration was done by Ito and Ikami (1984) in the neighboring part of Mizuho traverse route. A section was obtained between the route numbers S22 and S27-3 which are marked Ito and Ikami (1984) in Fig. 1. Their travel time curves did not show the apparent velocity of 4.7 km/s but showed the apparent velocity of 6.0 km/s in the same distance range from the shot point. This fact suggests that the velocity of 5.2 km/s in the second layer exists only locally near shot S-1. The estimated depth of the second layer coincides with the result of ice-radar sounding (Kamiyama *et al.*, 1994) as shown in Fig. 11. This fact also supports the existence of a discontinuity near shot S-1.

Thus, it is concluded that the depth of the upper boundary and the velocity of the second layer change rapidly in the neighborhood of the shot S-1. However, the bottom of the layer of 5.2 km/s is not identified in this study.

4.3. Discontinuity of the upper interface of the second layer near shot point S-4

As described above, a significant change of the thickness of the 3.8 km/s layer is estimated near shot point S-4. The location of the discontinuity coincides with the turning point of the trend of the free-air gravity in Abe (1975). This location also coincides with the echo-less points in the result of ice-radar sounding by Kamiyama *et al.* (1994).

Additional evidence of the significant discontinuity near the shot S-4 is described below. "Base altitude 3" is systematically underestimated between shots S-3 and S-4. "Base altitude 3" is a result for the pair of shot points S-3 and S-5. If this result is accepted, a discontinuity must be placed at shot point S-3. However, such a discontinuity is not acceptable because raw travel times around shot point S-3 are continuous as shown in Figs. 3 to 7 and 9. Thus such under-estimation between shots S-3 and S-4 and the apparent discontinuity around shot S-3 in "Base altitude 3" are considered to be artificial effects. The portion between shots S-3 and S-4 is not part of "Altitude (Final)" in Fig. 11.

The under-estimation only appears for the pair including shot S-4 in the middle. Therefore, it is suggested that the discontinuity near shot S-4 is significant and provides some kind of violation on the assumption of the analysis method.

The shape of the discontinuity still cannot be determined because the method of difference does not provide enough information to discuss it. The velocity change in the second layer across this discontinuity is not detected by this method.

5. Summary

The shallow structure of the earth's crust and its overlying ice-sheet down to 7 km depth is obtained with refraction analysis of the first arrival times observed during JARE-41. The first layer, with a uniform velocity of 3.8 km/s, is inferred to be the ice-sheet. The second layer, with a velocity of 6.2 km/s, is inferred to be the surface layer of the continental crust. The thickness of the second layer is estimated as approximately 5 km. The third layer has a velocity of 6.5 km/s: the shape of the top interface of this layer cannot be determined.

Two anomalous changes in ice-sheet thickness are estimated near shots S-1 and S-4. For the former change near shot point S-1, both change of velocity and change of basement depth exist in the second layer. A different velocity of 5.2 km/s for the second layer is estimated in this segment; this velocity is considered to be that of basement rocks. The upper boundary of the second layer around S-1 deepens abruptly on the coastal side by approximately 0.5 km. The latter discontinuity corresponds to a junction of the two blocks of the first layer. Velocity change between both sides of this undulation is not detected, but the first layer is divided into two blocks at this discontinuity. The thickness of the first layer thickens inland in the first portion. In contrast, the thickness of the first layer is almost constant in the second portion.

Acknowledgments

The authors express their best wishes to the persons listed below who provided valuable assistance in this operation: M. Yanagisawa, T. Minta, Y. Shimoda, N. Imae, H. Yamashita, S. Nomoto, J. Matsunaga and members of JARE-40 and -41 (leaders H. Miyaoka for JARE-40, M. Ayukawa and K. Watanabe for JARE-41), icebreaker *Shirase* and her crew under captain S. Shigehara. We appreciate their patience and valuable cooperation. And special thanks to Profs. K. Kaminuma and K. Shibuya of NIPR for constructive discussion and encouragement. Some of the apparatus used in this study was provided by Prof. T. Iwasaki of the Earthquake Research Institute, University of Tokyo. Comments by anonymous referees were effective in improving this paper. Finally, we dedicate this paper to all those who supported all phases of our operation in and on the way to Antarctica.

References

Abe, Y. (1975): Gravity data. JARE Data Rep., **28** (Glaciology 3), 9–114.
Fujita, S., Maeno, H., Uratsuka, S., Furukawa, T., Mae, S., Fujii, Y. and Watanabe, O. (1999): Nature of

radio echo layering in the Antarctic ice sheet detected by two-frequency experiment. J. Geophys. Res., **104**, 13013–13024.

Hagiwara, T. (1938): Kibanmen no keisha ga ichiyô de nai baai no sôji-kyokusen kaisekihô. Jishin Series I, **10**, 463–468 (in Japanese).

Hiroi, Y., Shiraishi, K. and Motoyoshi, Y. (1991): Late Proterozoic paired metamorphic complexes in East Antarctica, with special reference to the tectonic significance of ultramafic rocks. Geological Evolution of Antarctica, ed. by M.R.A. Thomson *et al.* Cambridge, Cambridge Univ. Press, 83–87.

Ikami, A. and Ito, K. (1986): Crustal structure in the Mizuho Plateau, East Antarctica, by a two dimensional ray approximation. J. Geodyn., **6**, 271–283.

Ikami, A., Ichinose, Y., Harada, M. and Kaminuma, K. (1983): Field operation of explosion seismic exploration in Antarctica. Nankyoku Shiryô (Antarct. Rec.), **70**, 158–182 (in Japanese with English abstract).

Ishizawa, K. (1979): An Elastic wave velocity in the surface of ice sheet in Antarctica and surveys on ice quakes. Doctoral Thesis of Akita University (in Japanese).

Ito, K. and Ikami, A. (1984): Upper crustal structure of the Prince Olav Coast, East Antactica. Mem. Natl Inst. Polar Res., Ser. C, **15**, 13–18

Ito, K., Ikami, A., Shibuya, K., Kaminuma, K. and Kataoka, S. (1983): Field operation of explosion seismic exploration in Antarctica (second paper). Nankyoku Shiryô (Antarct. Rec.), **79**, 107–133 (in Japanese with English abstract).

Kamiyama, K., Furukawa, T., Maeno, H., Kishi, T. and Kanao, M. (1994): Glaciological data collected by the 33rd Japanese Antarctic Research Expedition in 1992. JARE Data Rep., **194** (Glaciology 21), 1–67.

Kanao, M. (1997): Variations in the crustal structure of the Lützow-Holm Bay region, East Antarctica, using shear wave velocity. Tectonophysics, **270**, 43–72.

Miyamachi, H., Murakami, H., Tsutsui, T., Toda, S. and Minta, T. (2001): A seismic refraction experiment in 2000 on the Mizuho Plateau, East Antarctica (JARE-41)— Outline of observations. Nankyoku Shiryô (Antarct. Rec.), **45**, 101–147 (in Japanese with English abstract).

Murakami, H., Tsutsui, T., Miyamachi, H., Toda, S., Minta, T., Yanagisawa, M., Shimoda, Y. and Imae, N. (2001): Seismic exploration in Mizuho route. Dai-41-ji Nankyoku Kansokutai Hôkoku (Record of JARE-41), Tokyo, Natl Inst. Polar Res. (in press)(in Japanese).

Shiraishi, K., Ellis, D.J., Hiroi, Y., Fanning, C.M., Motoyoshi, Y. and Nakai, Y. (1994): Cambrian orogenic belt in East Antarctica and Sri Lanka; Implications for Gondwana assembly. J. Geol., **102**, 47–65.

Tsutsui, T., Yamashita, M., Murakami, H., Miyamachi, H., Toda, S. and Kanao, M. (2001): Reflection profiling and velocity structure beneath Mizuho traverse route, East Antarctica. Polar Geosci., **14**, 212–225.

(Received February 5, 2001; Revised manuscript accepted May 16, 2001)